An early fault diagnosis method based on the optimization of a variational modal decomposition and convolutional neural network for aeronautical hydraulic pipe clamps

Yang Tongguang, Yu Xiaoguang[1]**, Li Guanchen, Dou Jinxin and Duan Baojia**

Institute of Mechanical Engineering, Liaoning University of Science and Technology, Liaoning, Anshan 114051, People's Republic of China

E-mail: yuxiaoguang58@163.com

CrossMark

Abstract

An intelligent fault diagnosis method based on optimal variational modal decomposition (VMD) and a convolutional neural network (CNN) is proposed to solve the problems of the early faults and typical fault characteristics of hydraulic pipe clamps in aero-engines. Firstly, a modified genetic algorithm is used to optimize the selection of variational modal decomposition parameters, and the optimized VMD is used to decompose the signal. Secondly, the IMF weight of CNN fusion feature information is used. Finally, the fault pattern recognition is carried by CNN, so as to realize the intelligent fault diagnosis of an air hydraulic pipeline clamp. Experimental results show that this method can not only effectively clamp the health condition while the fault type is used to identify the accuracy, but can also realize the clamp early fault diagnosis. At the same time, through the clamp health status and test data analysis of typical fault status, we found that the typical fault characteristic frequency band provides a reference for the fault diagnosis of aerial hydraulic pipe circuit clamps.

(Some figures may appear in colour only in the online journal)

1. Introduction

The aero-engine hydraulic pipeline system is known as the 'cardiovascular system', which is one of the most important parts of an aircraft engine accessory device [1]. Most of the pipelines are connected to each other through a clamp, while the clamp is an important component to enhance the pipeline stiffness and fix the pipeline position. For a long time, failure of the aero-engine outer clamp-pipe system caused by vibration has been one of the most important problems affecting the reliability of the engine [2, 4]. Therefore, it is of great significance to study the vibration failure mechanism of aeronautical hydraulic pipeline clamp and find out the early failure of the clamp accurately.

In recent years, in order to avoid the vibration failure of the clamp-pipe system, some research has been done on the mechanical parameters and the clamp-pipe system model of aero-engines. For example, Ulanov and Bezborodov [5, 7] used the hysteresis curve obtained by the test to obtain the clamp support stiffness and the damping energy dissipation

[1] Author to whom any correspondence should be addressed.

coefficient under a static load. Gao *et al* [8, 10] obtained the aircraft pipe clamp stiffness based on the test and simplified it into a spring support. The modal test agrees well with the simulation results. Tan *et al* [11] proposed a method for identifying and locating the loosening of hydraulic clamps based on strain mode, in view of the fact that due to the influence of environmental factors such as internal system vibration on the hydraulic pipeline, it is easy to cause the loosening of clamps, thus resulting in serious failures such as pipeline wear and fatigue fracture.

Because the aeronautical hydraulic clamp-pipe system has high complexity, high noise and a large number of interference characteristics, leading to clamp has the characteristics of non-linear and non-stationary vibration signal. Especially for early failure, its characteristic signal is weak and can be submerged in a lot of noise, therefore it is difficult to extract the effective fault information, and should be carried out at the same time in time domain and frequency domain analysis and processing [12]. At present, the adaptive time-frequency analysis methods mainly include empirical mode decomposition [13] and local mean decomposition [14], which have been widely used in the field of fault diagnosis. However, they have problems such as endpoint effect, mode aliasing and decomposition stopping criteria [15]. Variational mode decomposition (VMD) [16] is a new method of time-frequency decomposition, which can effectively overcome the above problems. It uses the concept of non-recursive framework, has the advantages of strong decomposition and fast computation and has been widely used in the field of fault diagnosis [17, 18]. However, this method has a serious disadvantage [19]. The number of modal decomposition k and penalty factor α in its parameters must be pre-set by experience, which will lead to over-decomposition or under-decomposition of the decomposition results if set incorrectly. Therefore, it is necessary to optimize the selection of k and α parameters in the VMD algorithm, for example [20], Shan *et al* proposed a combined method based on an improved variational mode decomposition (IVMD) and a hybrid artificial sheep algorithm (HASA) for rotating machinery fault diagnosis [21]. Fu *et al* proposed a novel measuring model for the vibrational trend of an HPG based on optimal variational mode decomposition (OVMD) and a least squares support vector machine (LSSVM) improved with chaotic sine cosine algorithm optimization (CSCA).

Considering the characteristics of complexity and the intelligence of the aero-engine hydraulic pipeline, as well as its 'big data' feature, it is difficult for the traditional data method to meet the requirements of actual diagnosis [22]. Therefore, this paper proposes an improved genetic algorithm based on optimization of variational mode decomposition combined with convolution neural network intelligent fault diagnosis methods. First of all, for the band low signal-to-noise ratio and the vibration signal of the characteristics of strong stability, to optimize the VMD as the vibration signal preprocessor, giving full play to the advantages of good noise robustness. Secondly, selecting the fault feature information according to the correlation coefficient criterion, obviously the IMF component, through CNN adaptive fusion of IMF component

information, intelligent classification and identification of clamp faults are completed. Finally, this method is compared and analyzed with other fault diagnosis methods through test data. The results show that the performance of the fault diagnosis method proposed in this paper is obviously superior to the traditional intelligent identification method of back propagation neural network (BPNN). Moreover, the accuracy is higher than that of the current CNN diagnosis method.

2. Fundamental theory

2.1. Variational mode decomposition

Variational mode decomposition achieves effective signal decomposition by iteratively searching for the optimal solution of the variational model [23]. The process of constructing and solving the constrained variational model to complete signal decomposition involves the Wiener filter, Hilbert transformation and frequency mixing, etc, and the variational constraint problem is expressed as

$$\min_{\{\mu_k\},\{\omega_k\}} \left\{ \sum_{k=1}^{K} \left\| \partial_t \left[\left(\delta\left(t\right) + \frac{j}{\pi t} \right) * u_k\left(t\right) e^{-j\omega k^t} \right] \right\|_2^2 \right\}$$
$$\text{s.t.} \sum_{k=1}^{K} u_k = f. \quad (1)$$

In the above equation, $\delta\left(t\right)$ is the Dirichlet function, k is the number of components, $u_k = \{u_1, \cdots, u_k\}$ modal components of VMD decomposition, $\omega_k = \{\omega_1, \cdots, \omega_k\}$ represents the combination of the central frequencies of the K modal components and f represents the input signal. By introducing the quadratic penalty factor α and Lagrange multiplication operator $\lambda\left(t\right)$, equation (2) is transformed into the frequency domain to be solved by using Parseval/Plancherel Fourier isometric transformation, finally, the updated expression of the kth mode is shown below:

$$\widehat{u}_k^{n+1}\left(\omega\right) = \frac{\widehat{f}\left(\omega\right) - \sum_{i<k} \widehat{u}_i^{n+1}\left(\omega\right) - \sum_{i>k} \widehat{u}_i^n\left(\omega\right) + \frac{\widehat{\lambda}\left(\omega\right)}{2}}{1 + 2\alpha\left(\omega - \omega_k^n\right)^2}. \quad (2)$$

For a composite signal, the VMD divides the frequency band according to the frequency characteristics of the signal, and the mode and the corresponding center frequency are constantly updated in the frequency domain, finally realizing the adaptive decomposition of the signal.

2.2. Genetic algorithm improvement

The genetic algorithm [24] is a global optimal probabilistic search intelligent algorithm based on natural selection and evolution mechanism. It is widely used in combinatorial optimization, machine learning, and other fields. Nevertheless, the high computation complexity in solving nonlinear [25, 26], for this defect genetic algorithm, this paper on the crossover and mutation operators of the genetic algorithm to improve the genetic algorithm, according to the rules of neighbor selection of $N/2$ high fitness individuals, using the improved genetic algorithm to optimize variational modal decomposition of
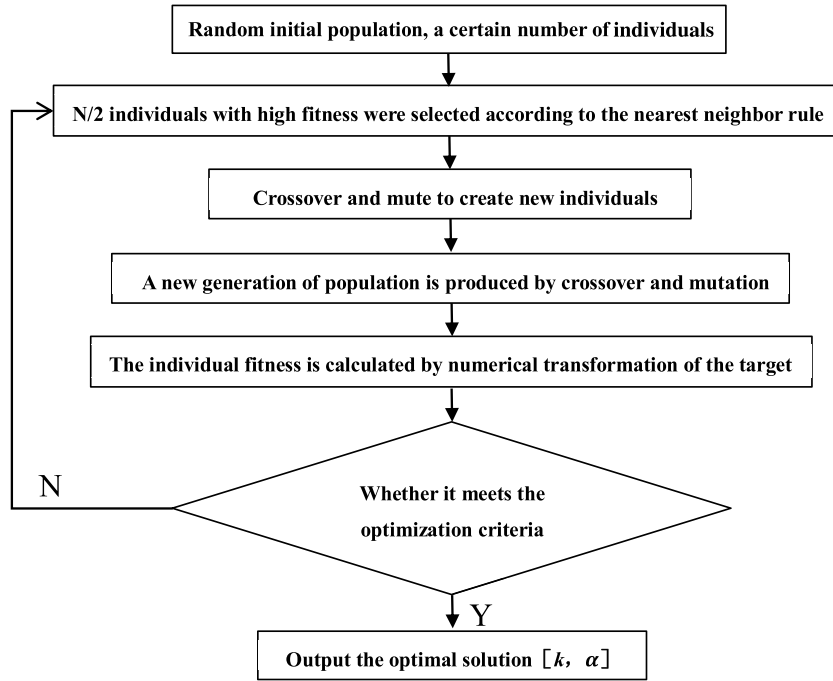
Figure 1. VMD parameter optimization based on the improved genetic algorithm.

modal number k value and penalty factor α values. Its specific implementation flow chart is shown in the figure 1.

2.3. VMD parameter optimization

According to the variational modal decomposition theory, the number of modal components k and penalty factor α should be set in advance when the VMD method decomposes signals. The k value determines the number of modes and center frequency, and α value is an important parameter to ensure the accuracy of VMD signal reconstruction [27, 28]. Before VMD decomposition, therefore, this article is based on the improved genetic algorithm, the use of marginal spectrum function as the criterion of the objective function in the global scope of parallel search solution space. In order to accurately obtain VMD $[k, \alpha]$ combination optimal parameters, so as to realize the adaptive weight number k and α value optimization algorithm, effectively avoiding caused by improper parameter combination set decomposition or weak fault features were drowned by the noise. Its specific flow chart is shown in figure 2.

2.4. Convolutional neural network

A convolutional neural network (CNN) is the true multi-layer structure learning algorithm in deep learning [29, 30], which is composed of the input layer, convolutional layer, pooling layer (also known as the sampling layer), fully connected layer and output layer. In recent years, CNN has become a leader in the field of deep learning with its extraordinary feature learning and pattern recognition ability, and has achieved a series of breakthroughs in the field of fault diagnosis [31, 34].
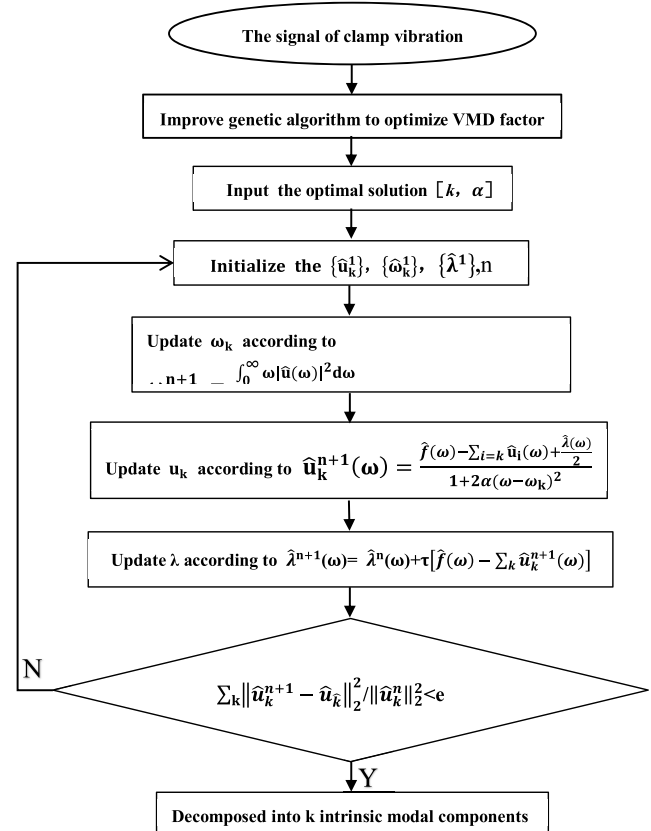

Figure 2. VMD decomposition flow chart based on modified genetic algorithm optimization.

2.4.1. Convolutional neural network (CNN). The convolutional layer (C layer) mainly performs feature extraction through feature maps of convolution check. In the process of
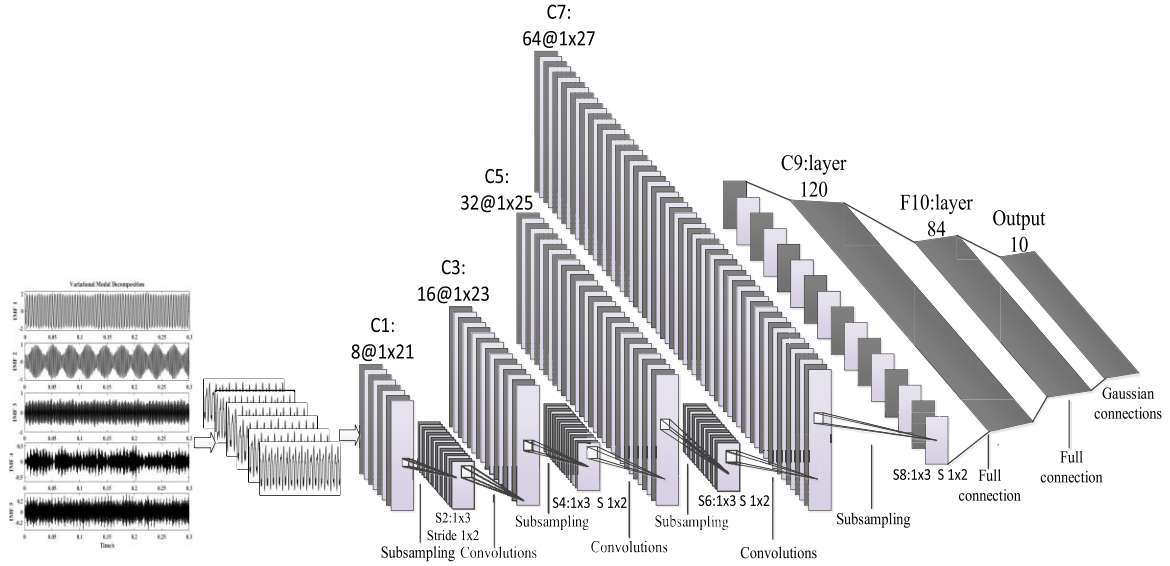
Figure 3. Structure design of the convolutional neural network.

convolution, this method has two characteristics: local perceptive convolution and weight sharing, which can greatly reduce the training parameters of the network [35]. The mathematical expression for the convolution process is as follows:

$$X_j^l = f \left(\sum_{i \in M_j} X_i^{l-1} \cdot \omega_{ij}^l + b_j^l \right). \tag{3}$$

In the above equation, X_j^l is the jth element in the l layer. M_j is the jth convolution region of $l-1$ layer feature graph. X_i^{l-1} is one of the elements. ω_{ij}^l is the weight matrix corresponding to the convolution kernel. b_j^l is the bias term. $f(\cdot)$ is the activation function, for which ReLU function is commonly used [36] and the mathematical expression is

$$f(x) = \max \left(0, \lg \left(1 + e^x \right) \right). \tag{4}$$

2.4.2. Pooling layer. The pooling layer (S layer) reduces the dimension of the feature graph, which guarantees the scale of the feature to some extent, and makes it have the invariance of scaling. The maximum pooling method has the best effect and is widely used. Its operation is shown in equation (5):

$$P^{1(i,j)} = \max_{(j-1)w < t < jw} \left\{ a^{1(i,t)} \right\} \quad j = 1, 2, \cdots, q. \tag{5}$$

In the above equation, $a^{1(i,t)}$ represents the tth neuron in the feature map of layer 1. w is the width of the convolution kernel, and j is the jth pool kernel.

2.4.3. Fully connected layer. The fully connected layer network classifies the extracted features. On the full connection layer, the input is obtained by weighted summation of all 1D feature vectors expanded by the feature graph and by activating the function

$$y^k = f \left(w^k x^{k-1} + b^k \right). \tag{6}$$

In the above equation, k is the serial number of the network layer. y^k is the output of the full connection layer. x^{k-1} is a 1D

eigenvector expanded. w^k is the weight coefficient. b^k is the bias term. Softmax is often used as the activation function $f(\bullet)$, which is an activation function for categorizing tasks. Finally, the output layer classifies and identifies the output features of the full connection layer [37].

2.5. Structure design of the convolutional neural network

Since the clamp vibration signal of aeronautical hydraulic pipeline is a 1D time series, this paper optimizes the typical convolutional neural network model to the 1D convolutional neural network model shown in figure 3. The optimized model consists of the input layer, CNN layer group, fully connected layer and output layer. The input is a 1D vibration signal. Since the learning ability of the convolutional neural network is positively correlated with the number of layers, the deeper the network structure, the stronger the feature learning and classification effect [38]. Besides, in order to effectively extract the information contained in the early fault signal of the clamp, a hidden layer is designed, which is composed of four layers of convolutional layers and four layers of sampling layers. To increase the nonlinear characteristics of the model [39], the most widely used ReLU (max (0, x)) function is adopted as the activation function. The maximum pooling method (max pooling) with the optimal pooling effect is selected for the pooling layer [40], that is, the maximum value in the $p \times p$ region is obtained for the feature map, on the condition that the region size is 1×2 and the regions do not overlap. The extracted characteristics are output by the Softmax classifier. Finally, according to the output result, the BP algorithm is used to update the weight and offset. According to the above basic principle of setting hyper parameters, a large amount of debugging is performed by using appropriate amount of sample data, and the appropriate parameters are finally obtained as shown in table 1.

In the above table, CW represents the convolution kernel width. CH represents the convolution kernel height. CC represents the current layer input feature map depth. CN represents the convolution kernel depth. S refers to the pooling band

Table 1. Main parameters of the CNN model.

Structure	Parameters
Convolutional layer	CW = 21; CH = 1; CC = 8; CN = 16; Strides:1
Pooling layer	S = 2
Convolutional layer	CW = 23; CH = 1; CC = 16; CN = 32; Strides:1
Pooling layer	S = 2
Convolutional layer	CW = 25; CH = 1; CC = 32; CN = 64; Strides:1
Pooling layer	S = 2
Convolutional layer	CW = 27; CH = 1; CC = 64; CN = 64; Strides:1
Pooling layer	S = 2
Fully connected layer	Number of nodes: 120, activation function: ReLU
Fully connected layer	Number of nodes: 84, activation function: ReLU
Dropout	Ratio: 0.15
Softmax	Output node: 10, activation function: Softmax

width. Strides represent the moving step of the convolution kernel. Feature integration is carried out on the designed CNN by four feature extraction units and two fully connected layers, and classification diagnosis is conducted through the Softmax layer. The convolution kernel size in each convolutional layer is 3 × 1, which realizes the deep structure of the network and improves the expressiveness of the network.

3. Fault diagnosis model of aeronautical hydraulic pipe clamps

The fault characteristic frequency of the aeronautical hydraulic pipeline clamp is affected by the complex structure, fluid-structure coupling vibration characteristics, strong noise interference and other factors, which results in the failure mechanism of the clamp being relatively complex and the early failure characterization is not obvious. At the same time, in order to facilitate the CNN model to study the characteristic of the signal, improve signal-to-noise ratio of the fault signal of the clamp, improve diagnosis accuracy, and satisfy the condition of small sample training. This paper presents a method combining variational modal decomposition and convolutional neural network based on the improved genetic algorithm to optimize VMD parameters, which is used to diagnose and identify the health state and different fault states of hydraulic pipeline clamps. The specific flow chart of fault diagnosis of the pipeline clamp is shown in figure 4. The specific steps are as follows.

(1) Signal acquisition and division: the clamped vibration signal is obtained by the acceleration sensor, and the sample signal is divided by windows of equal length. When the window moving step length is less than the signal length of a single sample, there will be overlaps between samples, and more samples can be extracted from signals of a fixed length, which is referred to as overlapped slices.

(2) Sample signal VMD decomposition: the sample signal obtained from vibration signal overlapping slices is VMD decomposition, and the original non-stationary signal $x(t)$ is decomposed into a series of stationary signals $c^{(1)}$, $c^{(2)}$, ···, $c^{(n)}$.

(3) Data set creation: stack the two IMF components with obvious fault characteristics into a multi-channel sample in a certain order, and increase the dimension of sample data by one dimension. The above operations are carried out for all sample signals to create the data set and divide the data set into a training set and test set.

(4) CNN design and training: CNN model was designed according to the design principles described in section 2.5, and the training set was used for training. CNN with good performance was obtained through a large number of tests and the debugging of various parameters.

(5) Qualitative diagnosis of the hydraulic pipe clamp fault: the effectiveness of the early fault diagnosis model based on optimized VMD and CNN was verified through the test set, and the training results of the model were compared with those of CNN and BPNN.

Using a new modern time-frequency analysis method, the vibration signal of complex clamps is pre-processed, which provides a good foundation for the learning of CNN model. Then, CNN is used to carry out adaptive fusion of each modal component, and the weight of each component fusion is obtained through training. Among them, parameters of the same input and output feature graph are shared, and neurons in the output feature graph are jointly determined by elements in the same position of each component.

4. The example analysis

4.1. Test instructions

The fault placement test is carried out for the hydraulic pipe clamp of the aero-engine. The data is collected and processed to verify the fault diagnosis method proposed in this paper. Figure 5 shows the hydraulic pipeline test device of the aero-engine, which is composed of an electric motor, plunger pump, frequency converter, throttle valve, oil tank, pipeline system and control system. The clamp used in the test is 304 stainless steel with a rubber strip, and the rubber material is FS6161 fluorosilicone gum rubber [41]. Artificial simulation tests on the clamp, a slightly loose, broken clamp pad, slight crack band root and other three kinds of typical early fault are used as embedded parts. Two acceleration sensors were used to collect the vibration data of the clamp synchronously in the straight pipe system and the bend pipe system, respectively. The test figures of the vibration test are shown in figures 6 and 7. The measurement positions were arranged as point 1 and point 2 from left to right, and the test parameter settings are shown in table 2.
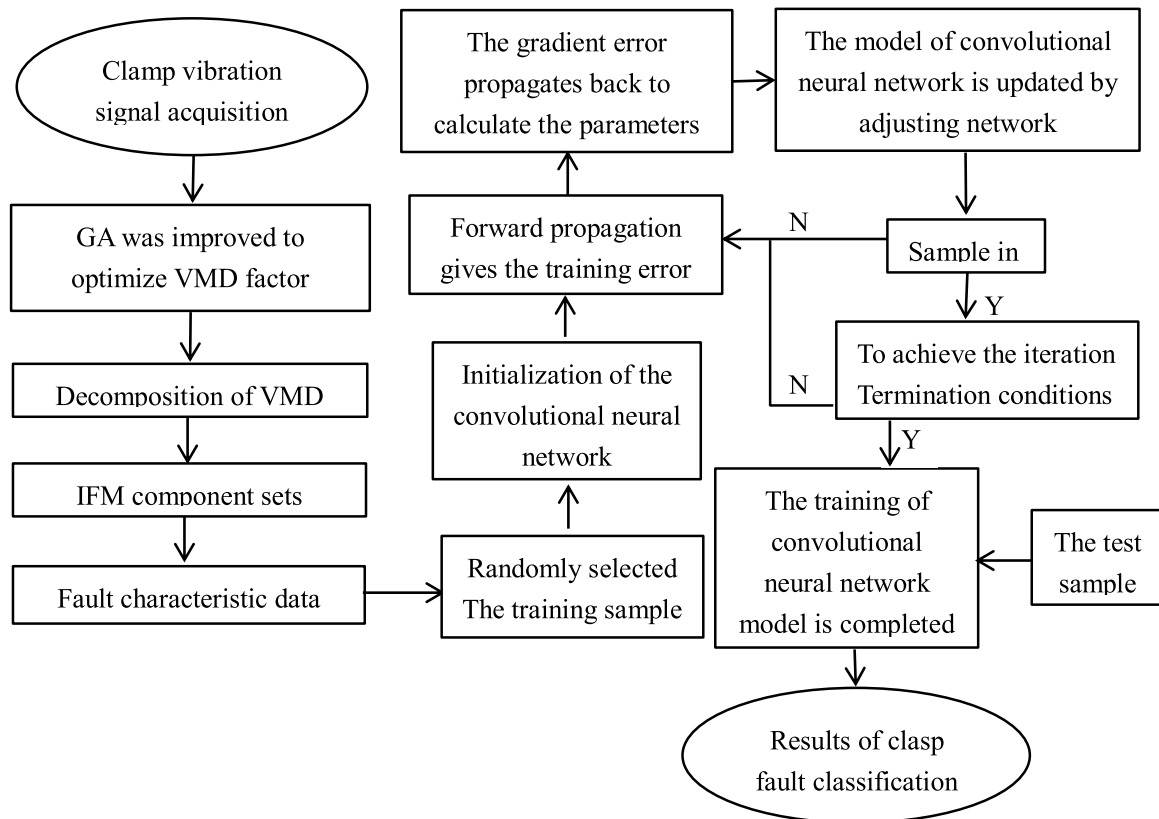
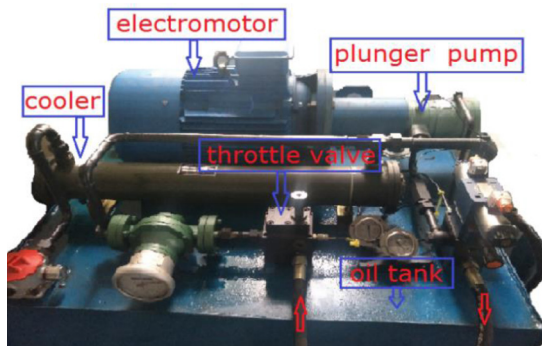**Figure 4.** Specific flow chart of clamp fault diagnosis.
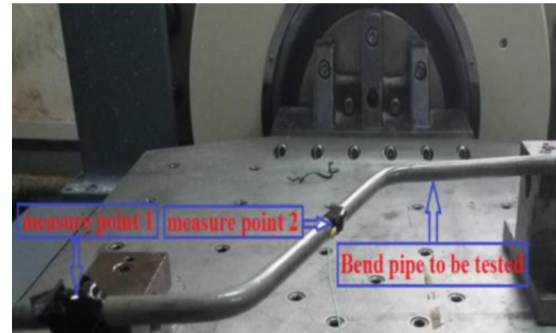

Figure 5. Hydraulic power system test equipment.
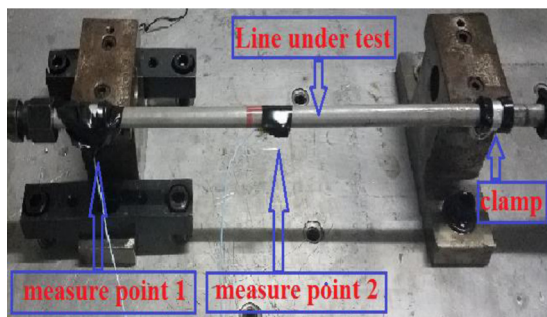

Figure 7. Bending clamp vibration test drawing.

Figure 6. Straight pipe clamp vibration test drawing.

Table 2. Test parameter setting table.

Parameter	Value of 1	Value of 2
Maximum pressure of hydraulic system	20 Mpa	
Hydraulic system test pressure	10 Mpa	
Maximum flow	39.2 l min^{-1}	
Motor speed	1500 r min^{-1}	1800 r min^{-1}
Sampling frequency	6400 Hz	

Time-domain vibration signals of the clamp in hydraulic elbow
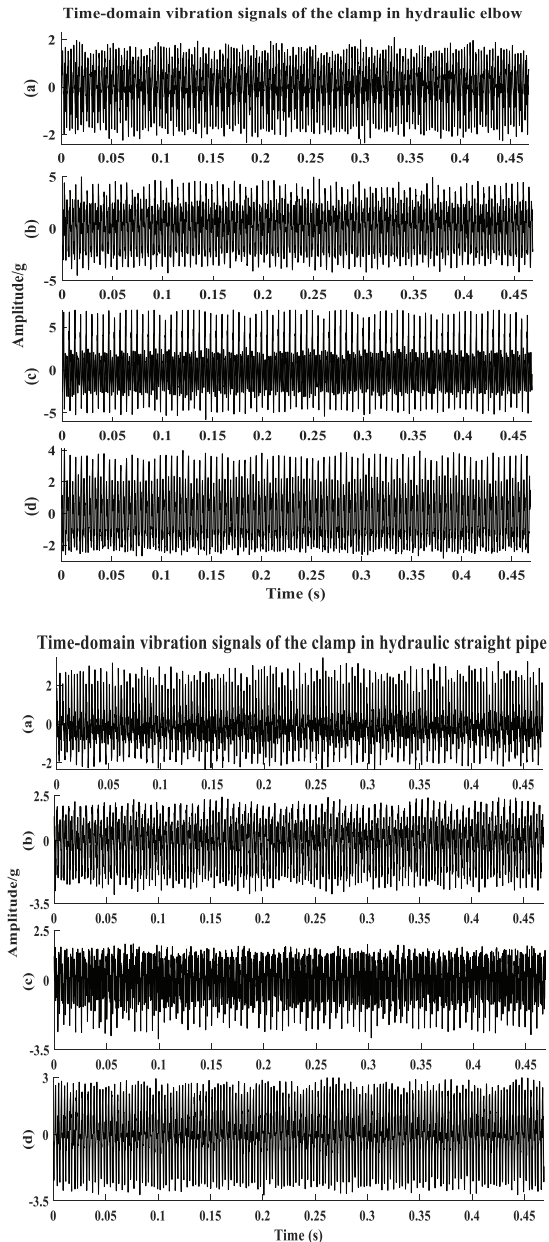

Figure 8. Time-domain of the clamp original vibration signal. (a) Clamp health condition. (b) Mild looseness of the clamp. (c) Pad wear of the clamp. (d) Slight crack of the clamp.

4.2. Data description

In order to verify the effectiveness of the method in the environment of a large amount of noise, Gaussian white noise of 20 dB and 50 dB was added into the test signal and constant frequency interference signal of 500 Hz was set to simulate the working state of the clamp in the actual project. After the noise is dyed, the clamped vibration signal collected from the measuring point 1 is used for this study. The time-domain waveform is shown in figure 8.

As can be seen from figure 8, by comparing the health state of the clamp and the time domain waveform of the three faults, it is found that the vibration amplitude of the early failure, such as slight looseness of the clamp, pad wear and a slight crack of the root, is increased relative to that of the health

state of the clamp, and the increase in amplitude is relatively significant. Besides, when the fault occurs, the amplitude of the bend pipe clamp fault is higher than that of the straight pipe clamp fault. Since the amplitude of slight looseness of the clamp is substantially the same as that of the wear of the clamp gasket, it is difficult to determine the fault type explicitly based only on the amplitude of the clamp fault.

4.3. Data processing

The vibration signal of the clamp health state and each fault state is processed according to the method described in section 3, and the optimal decomposition layer k of the variational mode decomposition is 4 and the penalty factor α is 1800. The original signal of the clamp is decomposed into four modal components, and different IMF components contain different time scales, so that the characteristics of the clamp signal can be displayed at different resolutions. In this paper, the vibration signal of the clamp health state and each fault including the slight looseness of the clamp, the wear of the gasket and the slight crack of the root are selected in the stainless steel hydraulic bend pipe structure, as shown in figure 9 after the improved VMD decomposition.

It can be seen from figure 9 that the adaptive decomposition of each modal function in the clamp vibration signal of the aeronautical hydraulic pipeline is realized by using the improved VMD method, and each component shows the modal characteristics of a certain scale range. The problems of end effect, modal aliasing and decomposition stop criterion are effectively avoided. Moreover, the improved VMD shows good noise robustness, and can effectively separate the added 500 Hz fixed-frequency interference signals. For example, the IMF2 component also verifies the feasibility of VMD decomposition layer number and penalty factor optimization selection based on the improved genetic algorithm, which reduces subjective errors of human factors and avoids excessive and insufficient signal decomposition. The frequency domain diagram of the clamp health state vibration signal is obtained by Fourier transform as shown in figure 10.

It can be seen from figure 10 that in both hydraulic straight pipe and bend pipe structure, the clamp vibration signal has a large amplitude at 355.3 Hz, which is more than 1400 g, and the amplitude is higher than that of other harmonic frequencies of the hydraulic system. According to the aero-engine hydraulic pipeline test system, the fundamental frequency of the hydraulic system is 178.2 Hz, and the frequency 355.3 Hz is twice the frequency of the hydraulic system. So 355.3 Hz is determined to be the characteristic frequency of the clamp. At the same time, the frequency domain diagram of the fault signals such as slight loosening of clamps, wear of gaskets and slight cracks at the root of the hydraulic bend pipe structure is as shown in figures 11–13.

As can be seen from figures 11–13, figure (a) is the frequency domain diagram of the original vibration signal of the clamp fault. Because the amplitude of the early fault signal will be very weak and seriously disturbed by noise, the characteristic frequency of the fault signal like clamp loosening will
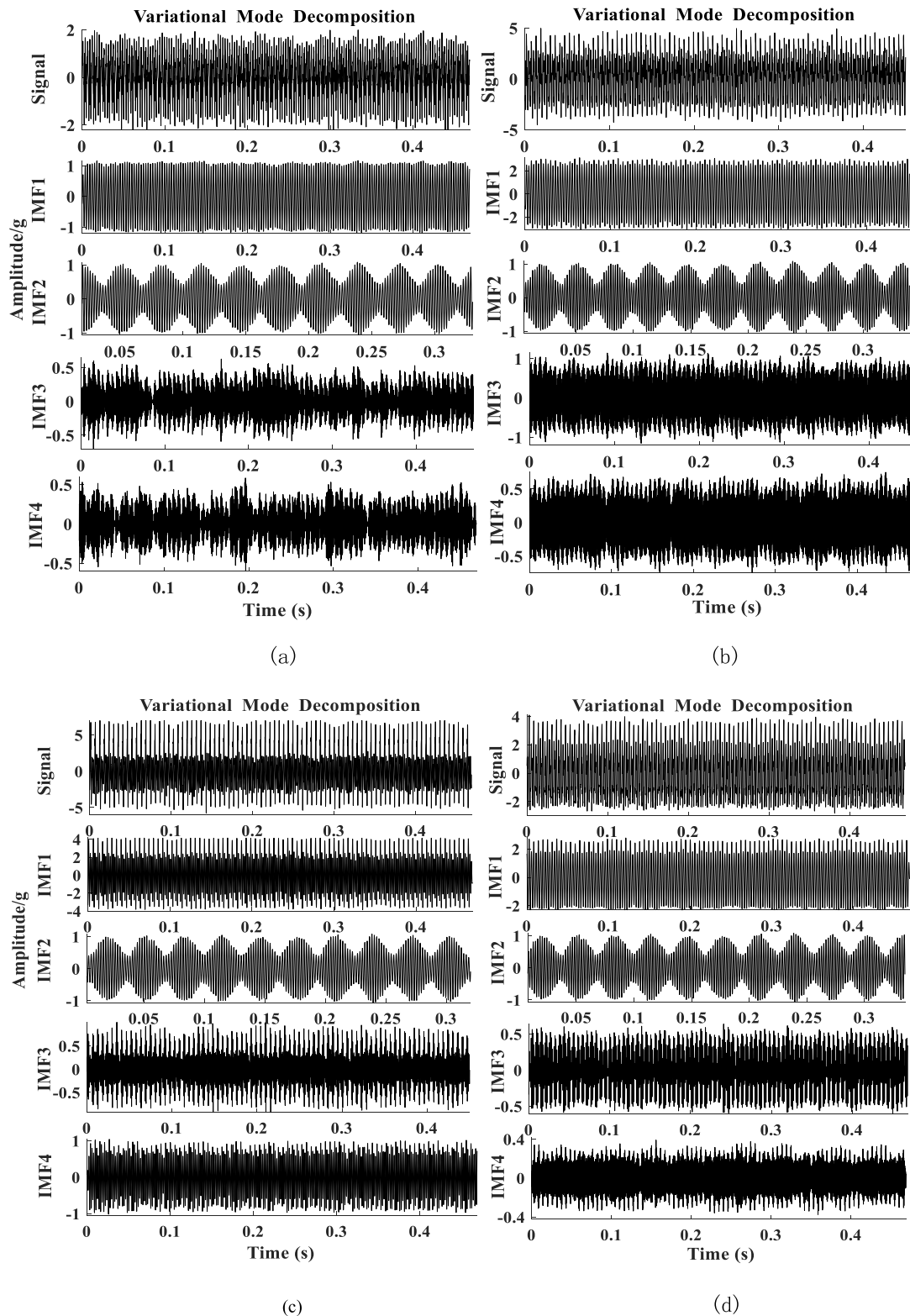
(a)

(b)

(c)

(d)

Figure 9. Time-domain of optimization VMD decomposition results. (a) Clamp health condition. (b) Mild looseness of the clamp. (c) Pad wear of the clamp. (d) Slight crack of the clamp.

be submerged in the harmonics of the system. Hence, it is difficult to find the fault characteristic law through the amplitude change. Therefore, this paper first carries on the VMD decomposition to the clamp fault vibration signal, and then according to the correlation coefficient principle, selects the component with larger coefficient value for reconstructing, so as to

improve the signal-to-noise ratio of the fault signal. Finally, by comparing the processed fault signal with the health signal, the typical fault characteristic frequency and the amplitude of the clamp are obtained, as shown in figure (b) and table 3.

From figure (b) in figures 11–13, it can be seen that the fundamental frequency of the hydraulic system is 178.2 Hz.
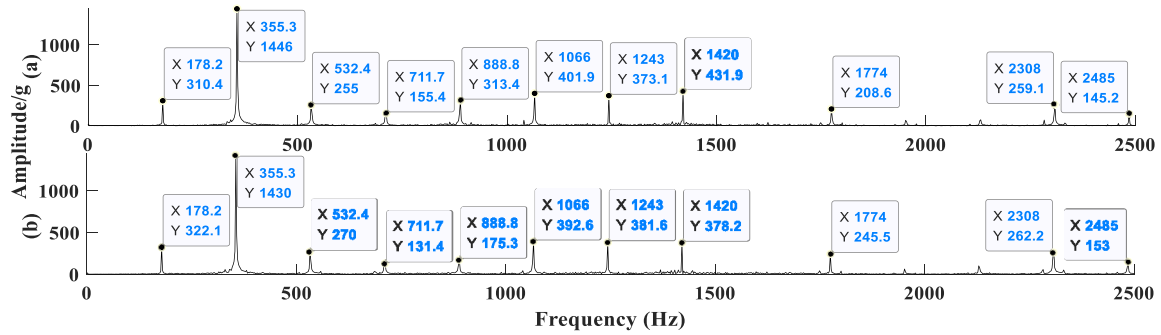
Figure 10. Amplitude spectrum of clamp health status. (a) Hydraulic elbow pipe. (b) Hydraulic straight pipe.

Table 3. Characteristic frequency of typical clamp faults.

Clamp state	Measure point	Fault frequency (Hz)	Amplitude (g)	3.5 times fault frequency (Hz)	Amplitude (g)	Clamp state	Fault frequency (Hz)	Amplitude (g)	3.5 times fault frequency (Hz)	Amplitude (g)
The elbow clamp	1	355.3	3848	1243	908	Mild loose of straight	355.3	1894	1243	390
Is mildly loose	2	355.3	3624	1243	718	Pipe clamp	355.3	1697	1243	386
The elbow clamp	1	533	3771	1243	535	Pad wear of straight	533	1071	1243	618
Is pad wear	2	533	3555	1243	572	Pipe clamp	533	1015	1243	753

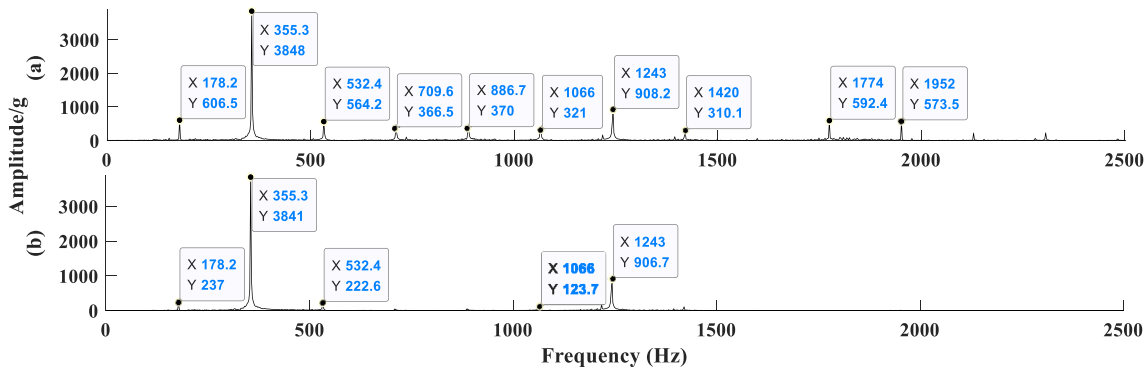| Clamp state	Measure point	Fault frequency (Hz)	Amplitude (g)	2.5 times fault frequency (Hz)	Amplitude (g)	Clamp state	Fault frequency (Hz)	Amplitude (g)	2.5 times fault frequency (Hz)	Amplitude (g)
The elbow clamp	1	355.3	2796	888.8	500	Slight crack of straight	355.3	2688	888.8	400
Is slightly cracked	2	355.3	2734	888.8	518	Pipe clamp	355.3	2675	888.8	396

Figure 11. Amplitude spectrum of clamp mild loosening. (a) Original signal. (b) After processing.

For clamp loosening, liner wear and root crack failure, the amplitude is reduced to 369 g, 1050 g and 396 g respectively after data processing. Besides, the amplitude noise reduction effect of other harmonic frequencies of the system is also significant, while the information of effective components is retained. From table 3, it can be seen that in the hydraulic bend pipe and straight pipe structure, through the comparative analysis of the amplitude of the clamp fault frequency collected by measuring point 1 and measuring point 2, it is

found that the fault frequency of slight loosening of the clamp is 355.3 Hz. And a large amplitude appears at the 1243 Hz, which is 3.5 times the natural frequency of the clamp. The fault frequency of clamp liner wear is 533 Hz, and there is also a large amplitude at 1243 Hz, which is 3.5 times of the natural frequency of clamp. The fault frequency of the slight crack at the root of the clamp is also 355.3 Hz, and a large amplitude appears at 888.8 Hz, which is 2.5 times the natural frequency of the clamp.
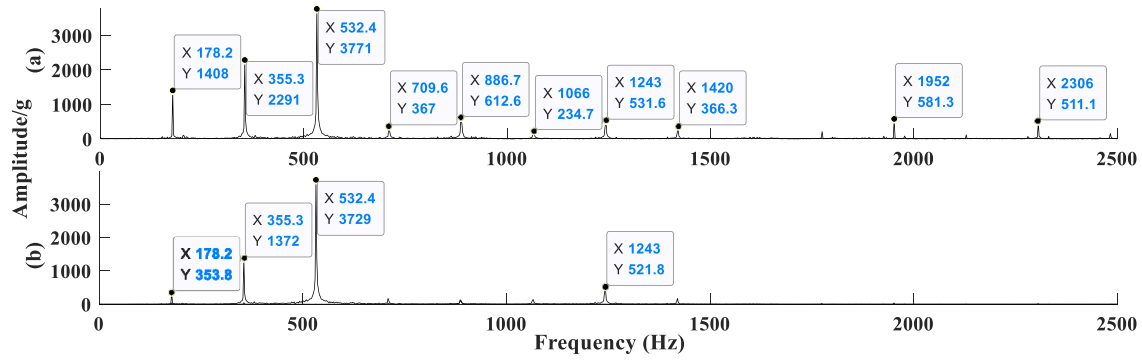
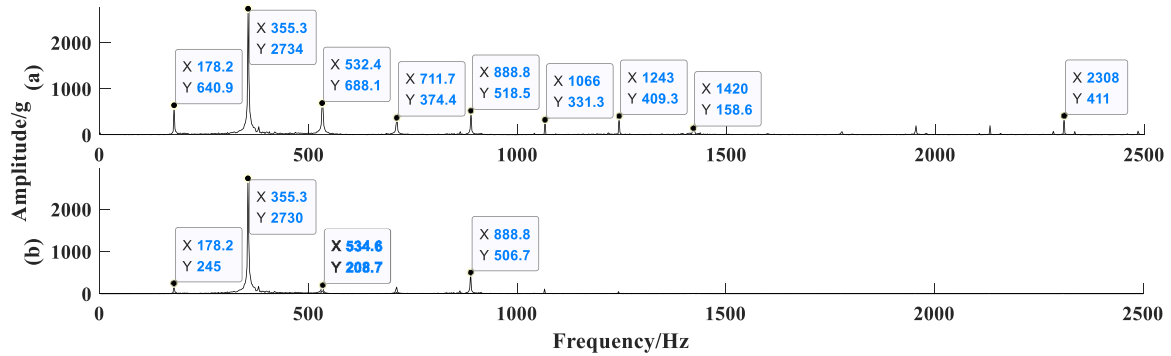**Figure 12.** Amplitude spectrum of clamp pad wearing. (a) Original signal. (b) After processing.

Figure 13. Amplitude spectrum of clamp slight cracking. (a) Original signal. (b) After processing.
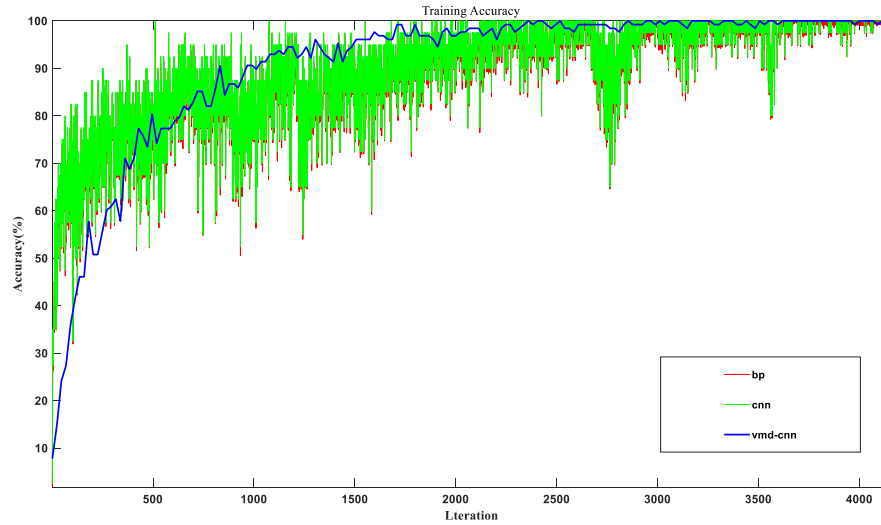

Figure 14. The iteration number and accuracy curve of clamp training.

4.4. Data set creation

Aviation band line fault feature information of the complex structure and fluid-structure coupling vibration characteristic factors leading to early failure characterization is not obvious. In order to avoid the failure information omission, this article will clamp fault features obvious to the IMF component in frequency since the childhood of the order stacked into multichannel samples. As shown in figure 3, each sample signal contains 3200 data points, and the data dimension of the sample is increased by one dimension. The data dimension of the sample changes from 1×3200 to $1 \times 3200 \times 2$

to create a data set, and the data set is divided into a training set and test set, the number of training samples in each state is 2000, and the number of predicted samples is 400. The proportion of the number of training samples to the number of forecast samples was 8:2. In order to verify the stability of the CNN model designed in this paper, the data set is trained by random sampling.

Based on the same data set, three methods, i.e. the improved VMD and CNN, CNN and BPNN, are used to diagnose the early fault of clamps. The relationship between the accuracy and loss rate of the data set and the number of iterations is shown in figures 14 and 15. Figure 14 shows that in the first
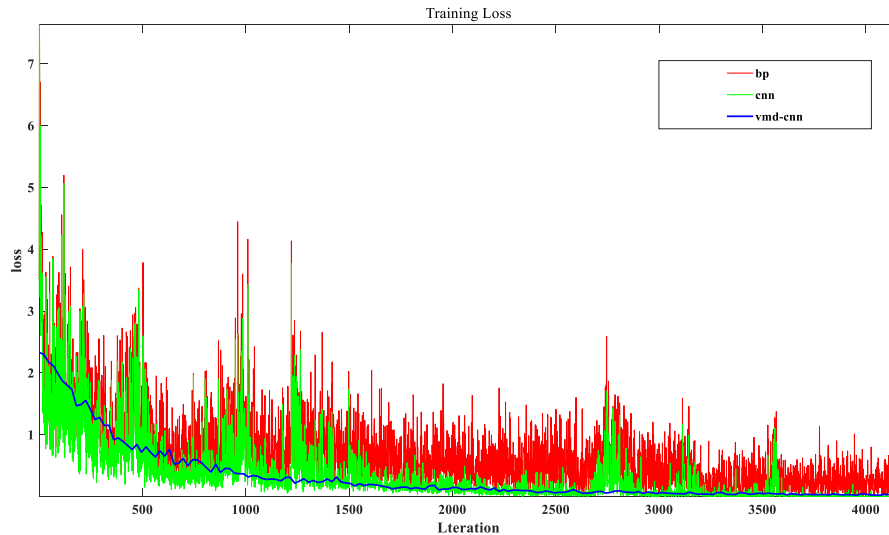
Figure 15. Iteration number and loss rate curve of hoop training.

Table 4. Description of a data set for hydraulic piping clamps.

Clamp state	Category labels	Number of measuring point	Measuring point location	Clamp state	Category labels	Number of measuring point	Measuring point location
The elbow clamp in normal condition	G1W	1	Clamp on the outer wall	Straight pipe clamp in normal condition	L1W	1	Clamp on the outer wall
The elbow clamp in normal condition	G1W-2	2	Line in the middle	Straight pipe clamp in normal condition	L1W-2	2	Line in the middle
The elbow clamp is mildly loose	G2S	1	Clamp on the outer wall	Mild loosening of the straight pipe clamp	L2S	1	Clamp on the outer wall
The elbow clamp is mildly loose	G2S-2	2	Line in the middle	Mild loosening of the straight pipe clamp	L2S-2	2	Line in the middle
The elbow clamp gasket broken	G4P	1	Clamp on the outer wall	Damaged ferrule lining of the straight pipe	L4P	1	Clamp on the outer wall
The elbow clamp gasket broken	G4P-2	2	Line in the middle	Damaged ferrule lining of the straight pipe	L4P-2	2	Line in the middle
The elbow clamp is slightly cracked	G3L	1	Clamp on the outer wall	Slight cracking of the straight pipe clamp	L3L	1	Clamp on the outer wall
The elbow clamp is slightly cracked	G3L-2	2	Line in the middle	Slight cracking of the straight pipe clamp	L3L-2	2	Line in the middle

1500 iterations, with the increase of the number of iterations, the accuracy of training using the improved VMD and CNN model is improved steadily. After 1500 iterations, the upward trend of accuracy slows down. It is basically stable, after 2000 iterations, and the prediction sample has a high accuracy, which can reach about 99%. The results show that the training model established in this paper has a strong ability to suppress over fitting, good stability and a good generalization ability for complex signal classification and diagnosis. On the other

hand, the accuracy of the CNN and BPNN diagnostic model training maintained an upward trend, but the training curve fluctuated greatly, and the accuracy of the clamp fault was about 90%.

As can be seen from figure 15, the loss value of training samples based on the optimized VMD-CNN model decreases and gradually approaches to zero with the increase of the number of iterations. After 2000 iterations, the loss of training samples is lower than that of CNN and BPNN, and the VMD-CNN model

MGA-VMD-CNN Confusion Matrix

Output Class	G1W-2	G1W	G2S-2	G2S	G3L-2	G3L	G4P-2	G4P	L1W-2	L1W	L2S-2	L2S	L3L-2	L3L	L4P-2	L4p	
G1W-2	12 / 3.0%																100% / 0.0%
G1W		32 / 8.0%															100% / 0.0%
G2S-2			12 / 3.0%														100% / 0.0%
G2S				28 / 7.0%													100% / 0.0%
G3L-2					36 / 9.0%												100% / 0.0%
G3L						36 / 9.0%											100% / 0.0%
G4P-2							16 / 4.0%										100% / 0.0%
G4P								24 / 6.0%									100% / 0.0%
L1W-2									32 / 8.0%								100% / 0.0%
L1W										20 / 5.0%							100% / 0.0%
L2S-2											28 / 7.0%						100% / 0.0%
L2S												24 / 6.0%					100% / 0.0%
L3L-2													30 / 7.5%	2 / 0.5%			93.8% / 6.3%
L3L														12 / 3.0%			100% / 0.0%
L4P-2															16 / 4.0%		100% / 0.0%
L4p															1 / 0.3%	39 / 9.8%	97.5% / 2.5%
	100% / 0.0%	100% / 0.0%	100% / 0.0%	100% / 0.0%	100% / 0.0%	100% / 0.0%	100% / 0.0%	100% / 0.0%	100% / 0.0%	100% / 0.0%	100% / 0.0%	100% / 0.0%	85.7% / 14.3%	94.1% / 5.9%	100% / 0.0%	100% / 0.0%	**99.3% / 0.7%**

Target Class

Figure 16. Based on MGA-VMD-CNN model with 16 kinds of aviation clamp.

tends to be stable. The results show that the training effect is ideal, and the actual output can approach the theoretical output well, which is suitable for the pattern recognition of early fault diagnosis of clamps. Due to the strong noise interference and the fluctuation of the loss value in the early training period of the BPNN network model, the CNN model can converge quickly after 2000 iterations, and the loss value approaches to zero slowly except in some nodes. However, the training convergence of the BPNN network model is poor and the stability is not high.

4.5. Results and analysis

4.5.1. Evaluating index. In order to measure the classification performance of the improved VMD and CNN models, four indexes including accuracy, precision, recall and F1-sore were calculated in this paper as evaluation indexes of classification performance.

4.5.2. Experimental result. A confusion matrix is a common visual tool in supervised learning, which can reflect the identification of each fault state more comprehensively. In this paper, each row in the matrix represents the prediction category of the data sample, and each column represents the actual category of the sample. The classification accuracy of each category can be clearly shown. The description of the hydraulic pipe clamp data set is shown in table 4.

As can be seen from figure 16, the accuracy of training results of the VMD-CNN diagnosis method by optimizing the data set composed of the clamp health state and three fault

CNN Confusion Matrix

Output Class	G1W-2	G1W	G2S-2	G2S	G3L-2	G3L	G4P-2	G4P	L1W-2	L1W	L2S-2	L2S	L3L-2	L3L	L4P-2	L4p	
G1W-2	12 / 3.0%																100% / 0.0%
G1W		32 / 8.0%															100% / 0.0%
G2S-2			12 / 3.0%														100% / 0.0%
G2S				28 / 7.0%													100% / 0.0%
G3L-2					36 / 9.0%												100% / 0.0%
G3L						36 / 9.0%											100% / 0.0%
G4P-2							16 / 4.0%										100% / 0.0%
G4P							4 / 1.0%	20 / 5.0%									83.3% / 16.7%
L1W-2									32 / 8.0%								100% / 0.0%
L1W										20 / 5.0%							100% / 0.0%
L2S-2											28 / 7.0%						100% / 0.0%
L2S												24 / 6.0%					100% / 0.0%
L3L-2													16 / 4.0%	16 / 4.0%			50.0% / 50.0%
L3L														12 / 3.0%			100% / 0.0%
L4P-2															1 / 0.3%	15 / 3.8%	6.3% / 93.8%
L4p															1 / 0.3%	39 / 9.8%	97.5% / 2.5%
	100% / 0.0%	100% / 0.0%	100% / 0.0%	100% / 0.0%	100% / 0.0%	100% / 0.0%	80.0% / 20.0%	100% / 0.0%	100% / 0.0%	100% / 0.0%	100% / 0.0%	100% / 0.0%	42.9% / 57.1%	50.0% / 50.0%	72.2% / 27.8%	**91.0% / 9.0%**

Target Class

Figure 17. Based on CNN model with 16 kinds of aviation clamp.

states listed in the figure is over 99.3%. The accuracy, precision and recall of the slight loosening fault and the slight crack fault of the clamp can reach more than 100%. In the straight pipe system, only for the single fault such as the slight
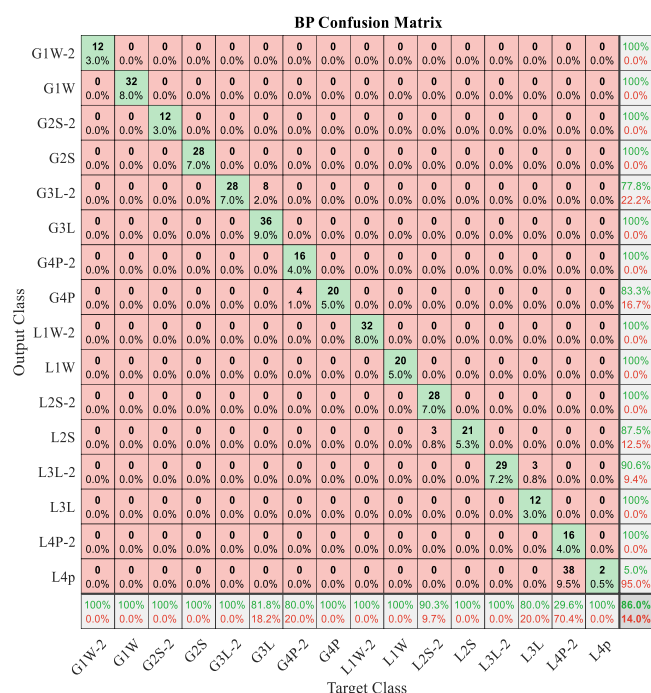
BP Confusion Matrix

Figure 18. Based on BPNN model of aviation clamps.

Table 5. The proposed method is compared with CNN and BPNN (%).

Evaluation index	VMD+CNN	CNN	BPNN
Accuracy	99.30	91.00	86.00
Precision	98.74	90.31	91.35
Recall	99.46	83.56	90.26
F1-sore	99.09	90.13	90.23

out for each method, and the average value of all kinds of evaluation indexes was used as the evaluation index of classified diagnosis performance of this method. It can be seen that the diagnosis accuracy of the diagnosis method based on optimized VMD and CNN is obviously better than the traditional diagnosis method of the typical shallow model BPNN. Compared with the deep convolution neural network used in recent years, all performance indexes of the method proposed in this paper can reach more than 98.7%, which is better than CNN, and it can also stably identify a variety of different health states of clamps. Compared with the CNN training model, the comprehensive accuracy is improved by 8.3%, while compared with the BPNN training model, the comprehensive accuracy is improved by 13%. The reason is that after optimizing VMD processing, the signal-to-noise ratio of the signal is improved and the over-fitting phenomenon is avoided. Moreover, the IMF feature components of all clamps are constructed as the multi-channel input of CNN, and the weight of each IMF feature component to the output is obtained adaptively by CNN information fusion.

5. Conclusion

(1) Aiming at the weak fault characteristics of the hydraulic pipeline clamp in an aero-engine, the strong nonlinear and unstable signals and the serious noise interference, in this paper, a fault diagnosis method based on optimized variational mode decomposition combined with a deep convolutional neural network is proposed to realize the adaptive diagnosis of clamp data.

(2) In order to solve the problem of a limited sample of clamp fault data acquired in engineering practice and preventing the CNN network model over fitting, in this paper, combining the advantages of VMD in signal processing and CNN's ability of independent learning data features and recognition, the intelligent early fault diagnosis of aeronautical hydraulic pipeline clamp is realized. Through the test, it is verified that the accuracy of the optimized VMD-CNN method can reach 99.3%, which is obviously better than the traditional BPNN diagnostic method, and higher than the CNN diagnostic method used in recent years. At the same time, VMD parameter factors are optimized based on the improved genetic algorithm to obtain the best combination of $[k, \alpha]$, which is verified in the clamp vibration signal.

(3) The vibration signals of clamp health state and typical faults are collected, compared and analyzed by the test method, and the characteristic frequencies of typical faults such as the slight loosening of clamps, wear of the clamp liner and slight cracks in the root of clamps can be found. It can provide a basis for early fault intelligent diagnosis of aeronautical hydraulic pipeline clamps.

cracking of the clamp and the wear of the gasket, the recognition rate is 85.7% and 94.1%, respectively. As a result, a 0.7% error rate is found in the comprehensive accuracy rate. At the same time, it also shows that the method proposed in this paper can accurately distinguish the early faults such as clamp loosening, cracking and so on. As can be seen from figures 17 and 18, the training based on the same data set through CNN and BPNN diagnosis methods shows the result that the average recognition rate for single faults such as the clamp slight cracking and clamp liner wear is about 50%. Among them, the recognition rate of the CNN network model for the clamp slight cracking fault at measuring point 1 in the straight pipe structure is only 42.9%, and the recognition rate of the BP network model for the clamp liner wear fault at measuring point 2 in the straight pipe structure is only 29.6%. As a result, the comprehensive accuracy was 91% and 86%, respectively.

Table 5 summarizes the comparison of training results of clamp fault data by using the method proposed in this paper, the CNN method and BPNN method based on the same data set. In order to avoid accidental error, 10 tests were carried

Acknowledgment

ORCID iDs

Yu Xiaoguang ⬤ https://orcid.org/0000-0003-1345-424X

References

[1] Zhaojun Z and Zhiying C 2011 Parametric modeling of clamps and influence of parameters on stiffness *J. Henan Univ.* **32** 13–5

[2] Zhanying L *et al* 2017 Responses of pipe system with flexible hoop under harmonic excitation *J. Aerosp. Power* **32** 2705–12

[3] Alizadeh A A, Mirdamdi H R and Pishevar A 2016 Reliability analysis of pipe conveying fluid with stochastic structural and fluid parameters *Eng. Struct.* **122** 24–32

[4] Tian J *et al* 2016 The vibration characteristics analysis of pipeline under the action of gas pressure pulsation coupling *Eng. Fail. Anal.* **16** 499–505

[5] Ulanov A M and Bezborodov S A 2016 Calculation method of pipeline vibration with damping supports made of the MR material *Proc. Eng.* **150** 101–6

[6] Bezborodov S A and Ulanov A M 2017 Calculation of vibration of pipeline bundle with damping support made of MR material *Proc. Eng.* **176** 169–74

[7] Ulanov A M and Bezborodov S A 2017 Research of stress-strained state of pipelines bundle with damping support made of MR material *Proc. Eng.* **206** 3–8

[8] Gao P *et al* 2016 A model reduction approach for the vibration analysis of hydraulic pipeline system in aircraft *Aerosp. Sci. Technol.* **49** 144–53

[9] Gao P *et al* 2018 Vibration and damping analysis of aerospace pipeline conveying fluid with constrained layer damping treatment *J. Aerosp. Eng.* **232** 1529–41

[10] Gao P *et al* 2019 Dynamic response analysis of aero hydraulic pipeline system under pump fluid pressure fluctuation *J. Aerosp. Eng.* **233** 1585–95

[11] Yuegang T *et al* 2017 Identification and location of hydraulic clamp looseness based on strain mode *Hydraul. Pneum.* **2017** 96–102

[12] Qingdong C *et al* 2019 Calculation of natural characteristics and experimental methods of the clamp-pipe system *J. Aerosp. Power* **34** 1029–35

[13] Junxun C *et al* 2017 Fault diagnosis of rolling bearing based on EMD *Vib. Impact* **36** 151–6

[14] Kang Z and Junsheng C 2016 Fault diagnosis of rolling bearing based on LMD and order tracking analysis *Vib. Test. Diagn.* **36** 586–91

[15] Yeh J R, Shieh J S and Huang N E 2010 Complementary ensemble empirical mode decomposition: a novel noise enhanced data analysis method *Adv. Adapt. Data Anal.* **2** 135–56

[16] Dragomiretskiy K and Zosso D 2014 Variational mode decomposition *IEEE Trans. Signal Process.* **62** 531–44

[17] Yang C and Jia M P 2019 A novel weak fault signal detection approach for a rolling bearing using variational mode decomposition and phase space parallel factor analysis *Meas. Sci. Technol.* **11** 115004

[18] Zhang M, Jiang Z and Feng K 2017 Research on variational mode decomposition in rolling bearings fault diagnosis of the multistage centrifugal pump *Mech. Syst. Signal Process.* **93** 460–93

[19] Wei D D *et al* 2019 An optimal variational mode decomposition for rolling bearing fault feature extraction *Meas. Sci. Technol.* **30** 055004

[20] Shan Y H *et al* 2019 A fault diagnosis method for rotating machinery based on improved variational mode decomposition and a hybrid artificial sheep algorithm *Meas. Sci. Technol.* **30** 055002

[21] Fu W L *et al* 2019 Vibration trend measurement for a hydropower generator based on optimal variational mode decomposition and an LSSVM improved with chaotic sine cosine algorithm optimization *Meas. Sci. Technol.* **30** 015012

[22] He K and Sun J 2015 Convolutional neural networks at constrained time cost *IEEE Conf. on Computer Vision and Pattern Recognition* (IEEE Computer Society) pp 5353–60

[23] Darong H, Lanyan K, Mengting L and Guoxi S 2019 A new method of bearing fault diagnosis based on VMD multi-scale entropy with parameter optimization *Control Decis. Mak.* **18** 11

[24] Singh A and Harshit X 2014 An enhanced area reduction technique for integrated circuit using genetic algorithm *IOSR J. Comput. Eng.* **16** 14–9

[25] Jun P, Sheng Ma Jiacheng H, Qingguo K and Long M 2018 Application of SVM optimized by genetic algorithm in aeroengine wear fault diagnosis *Lubr. Seal.* **43** 97

[26] Yan M F *et al* 2018 Improved adaptive genetic algorithm with sparsity constraint applied to thermal neutron CT reconstruction of two phase flow *Meas. Sci. Technol.* **29** 055404

[27] Mohanty S, Gupta K K and Raju K S 2018 Hurst based vibro-acoustic feature extraction of bearing using EMD and VMD *Measurement* **117** 200–20

[28] Chen L *et al* 2018 A seismic fault recognition method based on ant colony optimization *J. Appl. Geophys.* **152** 1–8

[29] Hinton G E and Salakhutdinov R R 2006 Reducing the dimensionality of data with neural networks *Science* **313** 504

[30] Lie Y *et al* 2015 A deep learning-based method for machinery health monitoring with big data *J. Mech. Eng.* **51** 49–56

[31] Zeng X, Liao Y and Li W 2016 Gearbox fault classification using S-transform and convolutional neural network *Int. Conf. on Sensing Technology* (IEEE) pp 1–5

[32] Janssens O *et al* 2016 Convolutional neural network based fault detection for rotating machinery *J. Sound Vib.* **377** 331–45

[33] Sun J, Xiao Z and Xie Y 2017 Automatic multi-fault recognition in TFDS based on convolutional neural network *Neurocomputing* **222** 127–36

[34] Aun W F *et al* 2017 An intelligent gear fault diagnosis methodology using a complex wavelet enhanced convolutional neural network *Materials* **10** 790

[35] Sun J *et al* 2015 Learning a convolutional neural network for non-uniform motion blur removal *Proc. of 2015 IEEE Conf. on Computer Vision and Pattern Recognition (Boston, MA)* (IEEE) pp 769–77

[36] Lei Y *et al* 2016 An intelligent fault diagnosis method using unsupervised feature learning towards mechanical big data *IEEE Trans. Ind. Electron.* **63** 3137–47

[37] Niaoqing H *et al* 2019 A planetary gearbox fault diagnosis method based on empirical mode decomposition and deep convolutional neural network *J. Mech. Eng.* **55** 9–18

[38] Sun W, Shao S and Yan R 2016 Induction motor fault diagnosis based on deep neural network of sparse auto-encoder *J. Mech. Eng.* **52** 65–71

[39] Luyang J *et al* 2017 An adaptive multi-sensor data fusion method based on deep convolutional neural networks for fault diagnosis of planetary gearbox *Sensors* **17** 414

[40] Wei Z, Gaoliang P and Chuanhao L 2017 *Rolling Element Bearings Fault Intelligent Diagnosis Based on Convolutional Neural Networks Using Raw Sensing Signal* (Cham: Springer)

[41] Wang Q *et al* 2017 Fault analysis and treatment of engine oil elbow clamp *Innov. Appl. Sci. Technol.* **2017** 71–2